Supplementary Information

for

Ribose-Ring Dynamics are Obligatory for Catalytic Function at the Active Site of the Lead-Dependent Ribozyme

Neil A. White[1†], Minako Sumita[1‡], Victor E. Marquez[2], and Charles G. Hoogstraten[1,*]

Table S1. Relaxation rates in the lead-dependent ribozyme. Transverse relaxation rates are listed at the nominal spin-lock power (ω_1). Dispersion plots (Figure 6, main text) were constructed and analyzed by calculating the effective spin-lock power ω_{eff} as the vector sum of ω_1 and the listed resonance offset.

			$R_{1\rho}$ (s^{-1})			
	|Offset| (Hz)	R_1 (s^{-1})	1.5 kHz	2.0 kHz	2.5 kHz	3.0 kHz
C2 C2′	560	2.44 ± 0.06	14.6 ± 0.7	13.3 ± 1.7	13.6 ± 0.7	13.0 ± 0.6
C5 C2 ′	544	1.43 ± 0.09	14.3 ± 2.9	23.6 ± 4.2	13.4 ± 1.9	13.3 ± 1.5
C6 C2 ′	487	1.45 ± 0.10	31.8 ± 5.5	28.7 ± 3.6	36.2 ± 6.8	35.2 ± 6.2
C6 C4 ′	526	1.23 ± 0.14	38.4 ± 5.6	36.4 ± 1.5	38.2 ± 6.3	31.0 ± 4.4
C10 C2 ′	543	2.47 ± 0.08	12.4 ± 1.3	12.0 ± 1.6	12.4 ± 0.8	13.5 ± 1.2
C10 C4 ′	514	1.55 ± 0.24	30.7 ± 4.4	42.0 ± 4.2	34.0 ± 4.9	28.8 ± 2.9
C11 C2 ′	554	1.83 ± 0.06	19.5 ± 0.9	15.1 ± 1.1	17.4 ± 0.8	17.5 ± 1.4
C14 C2 ′	503	2.71 ± 0.06	10.3 ± 0.5	13.2 ± 0.7	10.9 ± 0.6	11.0 ± 0.9
C28 C2 ′	560	2.38 ± 0.06	13.4 ± 0.8	13.3 ± 1.7	12.9 ± 0.7	13.3 ± 1.1
C30 C2 ′	240	1.91 ± 0.05	15.6 ± 1.4	12.4 ± 1.0	17.1 ± 0.9	15.9 ± 1.4
C30 C4 ′	643	1.83 ± 0.08	22.0 ± 2.4	22.8 ± 2.5	23.2 ± 1.8	23.7 ± 2.0

	$R_{1\rho}$ (s^{-1})					
Resonance	3.5 kHz	4.0 kHz	4.5 kHz	5.0 kHz	5.5 kHz	6.0 kHz
C2 C2′	12.6 ± 0.3	13.0 ± 0.4	12.3 ± 0.5	12.4 ± 0.8	12.2 ± 0.8	12.4 ± 0.2
C5 C2 ′	10.2 ± 1.14	12.0 ± 1.1	15.7 ± 3.0	15.3 ± 4.0	16.4 ± 9.5	17.2 ± 2.0
C6 C2 ′	29.6 ± 5.6	31.8 ± 6.4	29.8 ± 5.9	25.9 ± 3.8	34.8 ± 5.7	29.8 ± 5.3
C6 C4 ′	31.2 ± 5.6	33.9 ± 4.7	32.3 ± 6.6	26.6 ± 4.4	25.9 ± 4.0	25.8 ± 7.3
C10 C2 ′	12.7 ± 0.6	11.0 ± 0.7	11.0 ± 0.6	12.1 ± 0.9	11.6 ± 1.1	11.9 ± 0.7
C10 C4 ′	43.1 ± 4.0	30.5 ± 3.7	38.3 ± 6.5	27.1 ± 5.9	27.1 ± 5.9	31.5 ± 5.9
C11 C2 ′	16.4 ± 0.5	17.3 ± 0.9	16.0 ± 0.5	16.0 ± 1.5	16.1 ± 1.5	16.4 ± 0.5
C14 C2 ′	10.4 ± 0.3	10.3 ± 0.5	9.8 ± 0.6	9.4 ± 1.0	9.6 ± 0.7	10.1 ± 0.4
C28 C2 ′	13.2 ± 0.5	13.2 ± 0.5	12.2 ± 0.4	11.6 ± 1.1	12.4 ± 0.8	11.9 ± 0.4
C30 C2 ′	16.4 ± 0.3	16.1 ± 0.8	15.5 ± 0.6	14.9 ± 1.4	15.8 ± 1.1	16.3 ± 0.5
C30 C4 ′	20.2 ± 0.9	20.6 ± 1.3	20.5 ± 1.3	19.5 ± 2.0	18.5 ± 1.3	19.9 ± 1.2

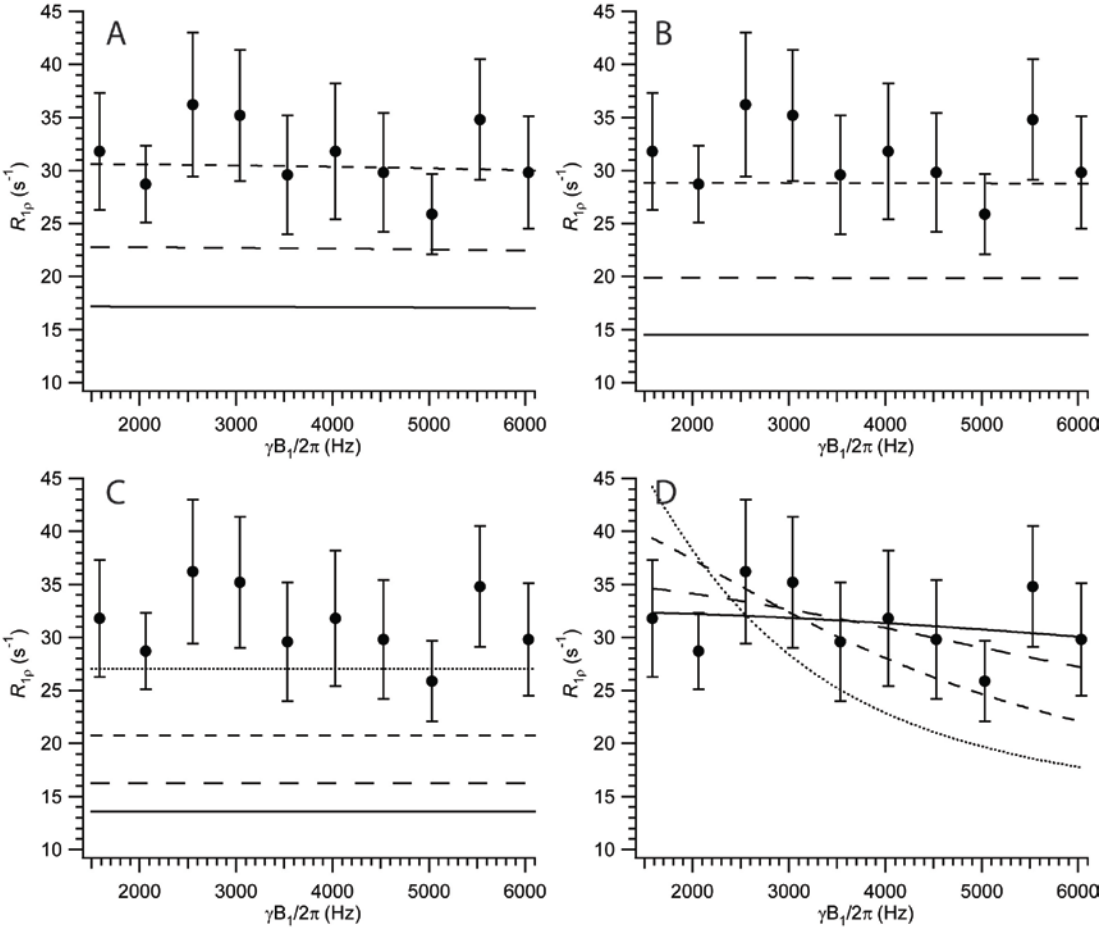

Figure S1. Determination of upper and lower bounds for exchange lifetime. Comparison of experimental data for C6 C2´ (main text, Figure 6) with: A), Simulated dispersion curves for τ_{ex} = 5 μs and $\Delta\omega_{min}$ = 2 ppm (solid), 3 ppm (long dash), 4 ppm (short dash); B), Simulated dispersion curves for τ_{ex} = 2 μs and $\Delta\omega_{min}$ = 2 ppm (solid), 4 ppm (long dash), 6 ppm (short dash); C), Simulated dispersion curves for τ_{ex} = 1 μs and $\Delta\omega_{min}$ = 2 ppm (solid), 4 ppm (long dash), 6 ppm (short dash), 8 ppm (dots); D), Dispersion curves at τ_{ex} = 10 μs (solid), 20 μs (long dash), 40 μs (short dash), 80 μs (dots) and the corresponding best-fit values of $\Delta\omega_{min}$. $R_{1\rho}°$ was set to 12.7 s^{-1} in all cases.